Photonic band gap properties of CdS-in-opal systems

A. Blanco, H. Míguez, F. Meseguer, C. López, F. López-Tejeira, and J. Sánchez-Dehesa

Photonic band gap properties of CdS-in-opal systems

A. Blanco, H. Míguez, F. Meseguer, and C. López[a)]
Instituto de Ciencia de Materiales de Madrid (CSIC), Cantoblanco 28049, Madrid, Spain and Unidad Asociada CSIC-UPV, Departamento Física Aplicada, Camino de Vera s/n, 46022 Valencia, Spain

F. López-Tejeira and J. Sánchez-Dehesa
Departamento de Física Teórica de la Materia condensada C-V, Universidad Autónoma de Madrid, Campus Cantoblanco, 28049, Madrid, Spain

Silica opals are used as templates where CdS is infiltrated with the aim to build inverse structures with enhanced photonic band gap properties. A control on the degree of infiltration, from 0% to 100%, is attained. The band gap at L is studied finding that the width decreases and then recovers as a function of CdS infilling (from bare opal to fully loaded structure). This is well accounted for by theory based on two different modes for the growth of CdS inside the opal pores. A shell mode seems to govern the growth at low infiltration (less than 10%). High quality opal templates, appropriate sintering, and a high and uniform infiltration are required to ensure further optical characterization of the inverse systems. Only heavily loaded structures are apt to be inverted. The gap in the fully loaded and the inverse opal are, respectively, two and three times broader than in the starting opal. © *2001 American Institute of Physics.* [DOI: 10.1063/1.1370981]

After some time has elapsed since they were first proposed,[1] there seems to be a clear-cut division in the approaches taken to obtain systems with an acceptable performance in photonic band gap engineering and technology. On the one hand, the methods derived from the microelectronics technology seem to yield very interesting results, mainly for two-dimensional systems, with the use of such techniques as photo- and electrolithography.[2] On the other hand, techniques based on self-assembly seem more appropriate for the formation of three-dimensional structures and make use of chemical and colloidal techniques. The latter are, in general, cheap, quick, and ready for large-scale reproduction; whereas the former are very laborious and expensive and require very modern technology not generally affordable. Synthetic opals are an example of the self-assembly approach that gained a great importance in the last few years because they have revealed as serious candidates to build up, at a very small expense, three-dimensional photonic crystals for the visible and near-infrared region of the electromagnetic spectrum.[3]

Although silica opals themselves have relatively modest photonic band gap properties due to both their structure (face centered cubic lattice) and material properties (reduced refractive index) the synthesis of guest materials within the intersphere cavity network can lead to an extraordinary enhancement of the photonic band gap properties. This enhancement is not limited to the formation of broad pseudogaps but may lead to a full photonic band gap development for sufficiently high dielectric contrast: 8.4.[4] In the optical range, this contrast is hardly achievable in loaded opals; not matter with what it is infiltrated. However, if the opal is removed from the composite the contrast (to vacuum, now) is more easily attainable and various materials qualify,

in particular, most of the technologically interesting semiconductors such as III–V and group IV. These structures are known as inverse opals and have been realized with various materials and by various methods. In this way, some recent experiments have shown very interesting results with TiO_2 (Ref. 5) and carbon[6] inverse opals. More recently, silicon inverse opals, with a dielectric contrast of about 12, have been realized with a complete band gap at 1.5 μm.[7] Germanium inverse opals have been fabricated in which a dielectric contrast of 16 will ensure the appearance of a complete photonic band gap in near-infrared.[8]

The aim of this work is to show a method to produce a CdS-based photonic crystal in which the photonic properties can be controlled by the degree of loading. The photonic band structure, in particular the lowest lying bands, are optically characterized and modeled. Although the luminescence of CdS is strongly altered in such systems,[9] it is not the goal of this letter.

The method of matrix preparation is based on natural sedimentation of silica nanospheres with a subsequent sintering process.[10] CdS is then synthesized in the opal voids by a chemical bath deposition method as previously reported.[9] Raman spectroscopy, x-ray diffraction, and scanning electron microscopy (SEM) have been used to characterize the semiconductor quality.[11]

Specular reflectance measurements allow us to follow the growth process and determine the CdS content, f, by fitting the positions of the first stop band at the L point through Bragg law. To estimate f we have linearly interpolated the dielectric constant of the composite. It is important to point out that, for later inversion, CdS content has to be as high as possible. Figures close to the available volume in the bare matrix, which is 26% for a compact fcc structure, are needed. This is a strong requirement if a self-standing inverse CdS structure is to be produced. Experimental results from reflectance measurements as a function of incidence

[a)]Author to whom correspondence should be addressed; electronic mail: cefe@icmm.csic.es
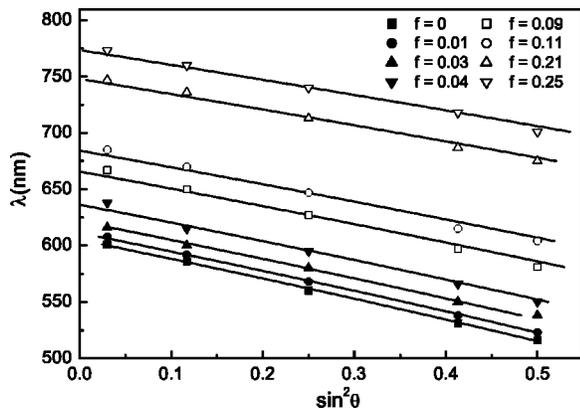
FIG. 1. Bragg peak position for bare and different CdS loaded opals of 275 nm spheres. Symbols represent experimental data and solid lines represent the fits to Bragg law.
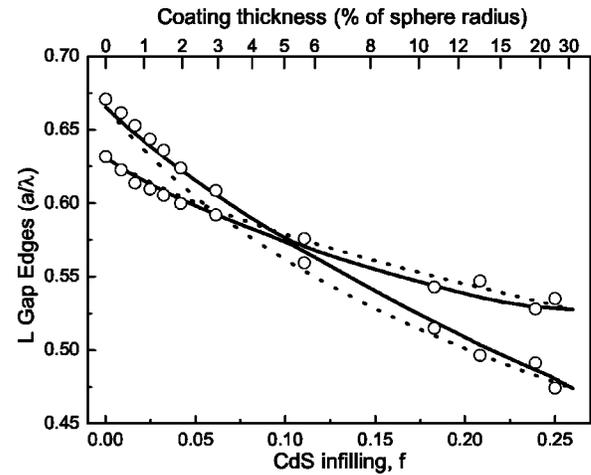

FIG. 2. Experimental L point stop band edges for the opal-CdS composites (circles) and theoretical predictions (lines). Homogeneous distribution model (dotted) and coating layer model (solid). Top axis shows, in percentage of the sphere radius, the layer thickness for the latter.

angle can be seen in Fig. 1 for a sample of 275 nm diameter spheres subjected to different treatments with increasing reaction times. CdS contents of about 3%, 9%, 16%, 32%, 42%, 80%, and 96% relative to the pore volume are found. Absolute infillings, f, are indicated in the labeling. In addition, data from the initial bare opal are shown. Let us not forget that the kind of characterization obtained by this means is macroscopic, the size of the probing beam being much larger than the microscopic features of the sample. This is particularly important for the highly infiltrated samples and means that high infill figures do not stem from local aggregations of CdS but from a uniform loading. Two important conclusions can be extracted from these data. First and most important: it is possible to infiltrate to almost 100% of the free volume; second: on loading, the composite keeps all of its photonic properties associated with the fcc arrangement along (111) direction.

We have studied the behavior of the L gap edges as the infiltration degree increases and both the dielectric contrast and the topology of the (more strongly) scattering matter change. The main finding is that the gap to midgap ratio decreases from about 6% in the original opal ($f=0$) to about 3% in half loaded structures ($f\approx0.1$) and then increases to ~12% for full infiltration while the gap center steadily decreases following the increase in average dielectric constant of the composite. Figure 2 shows the band edges at the L point versus the CdS filling fraction. Circles represent experimental data and lines theoretical predictions. Experimental data are obtained by plotting the energies, on either side of the peak, where reflectance takes one half of its maximum. The photonic band structures were obtained by solving the corresponding differential equation for electromagnetic wave propagation using a plane wave basis in an iterative implementation.[12] In order to simulate the dielectric distribution two semiconductor growth modes were considered. The first model (dotted line in Fig. 2) maps a homogeneous distribution of dielectric constant in the opal voids (with increasing value for increasing CdS content). The second one (continuous line in Fig. 2) assumes a layered growth such that the CdS forms shells that surround the opal spheres. An increase in CdS fraction means, in the first model, denser material filling the opal voids while, in the second one, thicker coating of the spheres. The first model is proposed

because the very early stages of the CdS growth, as microscopic characterization shows,[11] starts by forming nanometric grains in the space left by the silica spheres leading to a silica opal in which a mixture of CdS and air fills the pores. The second growth mode was observed for Si in this sort of open structures.[7]

In the early stages, the CdS growth seems to proceed by a shell thickening route (continuous line in Fig. 2). This behavior is, on the other hand, the only mechanism expected at very low infilling since new grains can only be formed on the surface of the spheres or on previously formed grains. For higher infiltrations ($f>0.1$), it is difficult to precise which mode is followed because of data scattering but clearly, the initial behavior is abandoned. This might be explained as follows. At first, grains of CdS nucleate on the spheres surface and cover the silica sphere in a layered growth. When the reaction time is longer a CdS network fills the opal voids, and small pockets of air are left empty. In this way, only very long exposures to the reactants can lead to a complete infiltration of the micropores. Another interesting feature that can be extracted from Fig. 2 is that, in the homogeneous model, the stop band at L vanishes when the average dielectric constant of the loaded voids (background) coincides with that of the silica ($\epsilon_s=2.1$) spheres and the composite becomes optically uniform. This can be written as $\epsilon_{pore}=1+f/0.26(\epsilon_{CdS}-1)$, where $\epsilon_{CdS}=5.75$.[13] Equating ϵ_{pore} to the silica dielectric constant yields $f=0.06$, very close to the value obtained from full theoretical calculations based on the first model ($f=0.055$). At this point, the dielectric contrast disappears and, consequently, no photonic crystal effects are expected. In the layered growth model, however, this cannot happen because of symmetry considerations: there cannot be four degenerate states in an anisotropic medium. At any rate, the fact that, for any filling ratio, the materials have precise boundaries and preserve the periodic structure at the relevant wavelength scale impedes the cancellation of dielectric contrast: an optically uniform medium is never obtained by increasing the thickness of the CdS layer. Notice that, as can be seen in Fig. 2, very thin layers are needed to achieve sizable infillings. The top axis presents the layer thickness
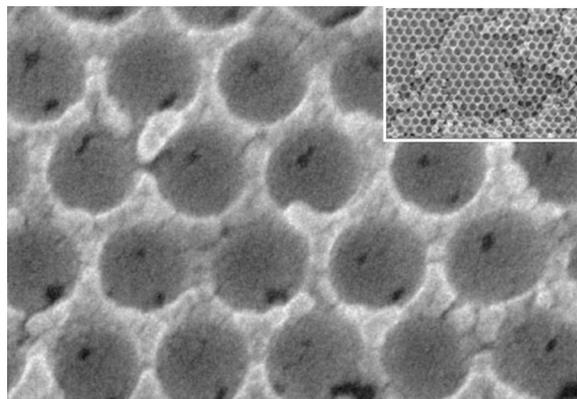
FIG. 3. SEM image of a (111) facet from a 275 nm spheres CdS inverted sample. The channels left by the sintering and through which the HF flows can be seen. The inset shows a lower magnification image where the overall structure is viewed.

FIG. 4. Reflectance at 10° incidence (solid lines) angle and theoretical position of the first stop band at the L point (shaded areas) for a 275 nm spheres opal.

for the corresponding filling ratio in units of the sphere radius. For instance at filling ratios less than 10% of the CdS layer is thinner than 5% of the radius which means, in practical terms, a few nanometers. This further supports the assumption that even in the case where growth is based on the formation of grains, the growth can only begin by a coating of the spheres.

Once nearly full CdS infiltration has been reached, the inversion of the structure can be tackled with all guarantees. To do that, the CdS/opal is immersed in a 1% diluted HF solution for about 6 h. For the success of this operation, it is very important that silica spheres are in contact with each other in order that HF flows throughout the structure. This requirement is fulfilled in sintered samples with a filling fraction of 0.74.[14] By this procedure, macroscopic samples (typically some millimeters) have been obtained in which optical measurements are performed. Figure 3 shows a typical SEM image of a (111) internal facet of CdS inverse opal (sphere diameter 275 nm) after cleavage. In the inset, the uniformity of the growth and that very high percentage of infilling achieved (virtually 100%, yielding a negative replica of the original opal) can be appreciated.

Optical properties of the samples thus obtained have been explored by means of reflectance (taken, for practical convenience, at 10° incidence) and compared with those of the original bare opal and infiltrated one. In Fig. 4 the reflectance at 10° incidence for a 275 nm sphere opal in its three states (bare, CdS infiltrated to 96%, and inverted) is plotted. The shadowed areas represent the predicted photonic pseudogap at the L point. Theoretical estimates are for bare opal (top), fully infiltrated (middle), and totally inverted (bottom). The agreement between theory and experiment is satisfactory. Starting from bare opal (silica-air), the gap to midgap ratio for this first pseudogap is about 6% with a refractive index contrast of 1.45; in the CdS-silica composite, the ratio is 12% and the contrast 1.7; finally, for the inverted structure, the ratio is 18% the contrast being 2.4. The increase measured in the final structure (three times with respect to the initial opal) is a huge enhancement of the photonic properties and very useful for systems in which a strong interaction is needed between the photonic structure and an active material therein. In the case of CdS, the semiconductor itself is the active material.
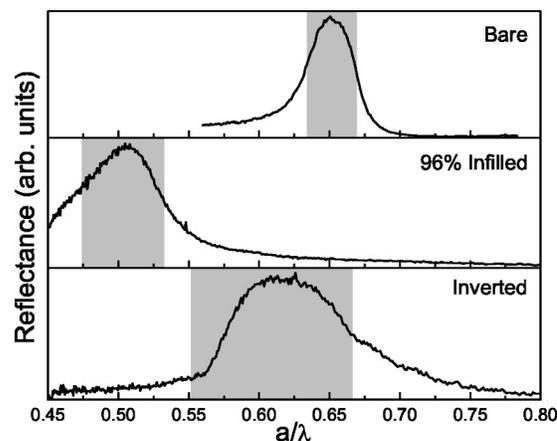
In summary, we have shown that it is possible to fabricate CdS inverse opals of high quality using a very cheap technique. As compared to the bare opal, the photonic properties are enhanced in the composite (gap width doubled) and more so in the inverse structure (gap width trebled). In addition, we have studied the first stop band as CdS infilling increases and it has been found that its width decreases and then increases in accord with theoretical models.

[1] E. Yablonovitch, Phys. Rev. Lett. **58**, 2059 (1987); S. John, *ibid.* **58**, 2486 (1987).

[2] S. Noda, A. Chutinan, and M. Imada, Nature (London) **407**, 608 (2000); E. Chow, S. Y. Lin, S. G. Jonson, P. R. Villeneuve, J. D. Joannopoulos, J. R. Wendt, G. A. Vawter, W. Zubrzycki, H. Hou, and A. Alleman, *ibid.* **407**, 983 (2000).

[3] H. Míguez, C. López, F. Meseguer, A. Blanco, L. Vázquez, R. Mayoral, M. Ocaña, V. Fornés, and A. Mifsud, Appl. Phys. Lett. **71**, 1148 (1997).

[4] K. Busch and S. John, Phys. Rev. E **58**, 3896 (1998).

[5] J. E. G. J. Wijnhoven and W. L. Vos, Science **281**, 802 (1998).

[6] A. A. Zakhidov, R. H. Baughman, Z. Iqbal, C. Cui, I. Khayrullin, S. O. Dantas, J. Marti, and V. G. Ralchendo, Science **282**, 897 (1998).

[7] A. Blanco, E. Chomski, S. Grabtchak, M. Ibisate, S. John, S. W. Leonard, C. López, F. Meseguer, H. Míguez, J. P. Mondia, G. Ozin, O. Toader, and H. M. van Driel, Nature (London) **405**, 437 (2000).

[8] H. Míguez, F. Meseguer, C. López, M. Holgado, G. Andreasen, A. Mifsdu, and V. Fornés, Langmuir **16**, 4405 (2000).

[9] A. Blanco, C. López, R. Mayoral, H. Míguez, F. Meseguer, A. Mifsud, and J. Herrero, Appl. Phys. Lett. **73**, 1781 (1998).

[10] R. Mayoral, J. Requena, J. S. Moya, C. López, A. Cintas, H. Míguez, F. Meseguer, L. Vázquez, M. Holgado, and A. Blanco, Adv. Mater. **9**, 257 (1997).

[11] R. Torrecillas, A. Blanco, M. E. Brito, C. López, H. Míguez, F. Meseguer, and J. S. Moya , Acta Mater. **48**, 4653 (2000).

[12] R. Maede, A. M. Rappe, K. D. Rommer, and J. D. Joannopoulos, Phys. Rev. B **48**, 8434 (1993); S. G. Johnson, *ibid.* **55**, 15942 (1997). We acknowledge MIT photonic band package for photonic band structure calculations.

[13] The CdS refractive index used in the calculation is a mean value $n_{CdS} = 2.4$. It ranges from 2.5 to 2.3 for wavelengths between 400 and 800 nm.

[14] M. Míguez, F. Meseguer, C. López, A. Blanco, J. S. Moya, J. Requena, A. Mifsud, and V. Fornés, Adv. Mater. **10**, 480 (1998).